Classification:

Major: Physical Sciences

Minor: Biochemistry

TITLE

Kinetic barriers to SNAREpin assembly in the regulation of membrane docking/priming and fusion

AUTHORS

Feng Li,[1] Neeraj Tiwari,[1] James E. Rothman[1,*] and Frederic Pincet[1,2,*]

AUTHOR AFFILIATIONS

[1]Department of Cell Biology, School of Medicine, Yale University, 333 Cedar Street, New Haven, CT 06520, USA

[2]Laboratoire de Physique Statistique, UMR CNRS 8550 associée aux Universités Paris 6 et Paris 7, Ecole Normale Supérieure, 24 rue Lhomond, 75005 Paris, France

*Correspondence to: James E. Rothman (james.rothman@yale.edu) and Frederic Pincet (pincet@lps.ens.fr)

KEYWORDS

SNARE, zippering, energy landscape, Readily Releasable Pool (RRP) refilling, Complexin, Synaptotagmin, Munc18, Tomosyn, regulatory machinery organization.

ABSTRACT

Neurotransmission is achieved by SNARE-driven fusion of readily-releasable vesicles that are docked and primed at the presynaptic plasma membrane. After neurotransmission, the readily-releasable-pool of vesicles must be refilled in less than *100 ms* for subsequent release. Here we show that the initial association of SNAREpins is far too slow to support this rapid refilling owing to an inherently high activation energy barrier. Our data suggest that acceleration of this process, *i.e.* lowering of the barrier, is physiologically necessary and can be achieved by molecular factors. Furthermore, under zero force, a low second energy barrier transiently traps SNAREpins in a half-zippered state similar to the partial assembly that engages calcium-sensitive regulatory machinery. This suggests that the barrier must be actively raised *in vivo* to generate a sufficient pause in the zippering process for the regulators to set in place. We show that the heights of the activation energy barriers can be selectively changed by molecular factors. Thus, it is possible to modify, both *in vitro* and *in vivo*, the lifespan of each metastable state. This provides a simple model in which vesicle docking/priming, an intrinsically slow process, can be substantially accelerated. It also explains how the machinery that regulates vesicle fusion can be set in place while SNAREpins are trapped in a half-zippered state.

SIGNIFICANCE STATEMENT

Neurotransmission requires fusion of the synaptic vesicles that are closely apposed to the presynaptic membrane. This apposition is achieved through the initial association of proteins known as SNAREs. After a neurotransmission event, other vesicles must be rapidly prepared for the next round of fusion. Here we find the kinetics of the initial formation of SNARE complexes is too slow to spontaneously achieve this process because of a high activation energy barrier, but can be accelerated by molecular factors. In addition, we show that a second energy barrier transiently traps the SNARE complexes in a half zippered state. This pause provides time for the regulatory machinery that accurately controls synchronized neurotransmission to be set in place.

\body

INTRODUCTION

In synaptic transmission, neurotransmitter-containing vesicles are docked and primed at the presynaptic plasma membrane forming a readily releasable pool (RRP). Priming is achieved through partial association of v-SNAREs (soluble NSF attachment protein receptor) from the vesicle with t-SNAREs from the plasma membrane at their N-terminal subdomains. The vesicles discharge their contents into the synaptic cleft upon stimulation by elevated intracellular Ca^{2+} influx.(1) After the vesicles release their cargo, a new batch of vesicles docks to the presynaptic membrane and their v-SNAREs associate with t-SNAREs to be primed for the next round of fusion(2, 3). This process refills the RRP. At fast synapses, the rate of vesicle refilling is ~100 *ms*.(4-6) The assembly of the fusion-competent protein complex includes the N-terminal association of the t- and v-SNAREs, and thus this association must occur within such a timeframe.(1, 7-10) In the conventional progressive zippering model, the N-terminal layers of the SNAREs have been presumed as the point where the assembly process is started, and hence has been thought to be rapid.(11) However, recent studies show the N-terminal assembly has to reach the middle layers (around layer -1) to achieve meaningful binding affinity; zippering of this subdomain is the rate-limiting step of membrane fusion and takes minutes.(12) How can these two time-scales, 100 *ms* and minutes, be reconciled? Here we precisely quantify the rate of assembly and show that the slow rate of N-terminal zippering is due to a high activation energy barrier that has to be overcome. Previous reports indicated that fusion can be accelerated in vitro by pre-incubating the t-SNARE with the C-terminal region of the v-SNARE. (11, 13) We demonstrate that this acceleration is due to a structural change of t-SNARE which results in lowering of the activation energy barrier and faster N-terminal assembly. We find that this acceleration is a general feature that can be achieved by other protein factors.

After the N-termini of the SNAREs have assembled, their C-terminal regions have to further zipper up and provide enough energy to the membranes to induce fusion. Functionally, these two assembly steps are distinct.(12) However, it remains unclear whether they are kinetically separated, i.e. whether there is a pause in the assembly process between them. Some biophysical studies have tackled this issue.(9, 14-17) Notably, when a single SNARE complex is disassembled with optical tweezers, extrapolation of the applied force to zero leads to a continuous downhill energy landscape which prevents any pause.(15) Synaptic vesicle fusion is

strictly regulated by neuronal proteins such as Complexin and Synaptotagmin. Evidences suggest that these regulators may act on the half-zippered SNARE.(17-20) Therefore, a kinetic pause between the N- and C-terminal zipperings would be a key factor for organizing the regulation machinery. Here, we establish the existence of this kinetic pause between the two assembly steps under zero force.

RESULTS

N-terminal assembly is thermodynamically favorable, but kinetically unfavorable

To study the initial assembly of the v-SNARE (VAMP2) and t-SNARE (a complex of Syntaxin1A and SNAP25), we first measured the interactions between the N-terminal peptide of VAMP2 (Vn peptide, VAMP2 residues 1 to 57) and the entire cytosolic domain of t-SNARE (Syntaxin1A residue 1 to 265 and SNAP25 residues 1 to 206, Figure 1A) using Isothermal Titration Calorimetry (ITC). Surprisingly, when Vn was titrated into t-SNARE solution, the heat spikes had the same amplitude as in water-water titration, indicating that no binding signal was detected (Figure 1B). This was unexpected because the binding between the t- and v-SNARE is mainly due to exothermic hydrophobic interactions between heptad repeat motifs.(21, 22)

We also separately titrated the C-terminal subdomain of v-SNARE (Vc peptide, VAMP2 residues 58 to 94) and the entire cytosolic domain (CDV, VAMP2 residues 1 to 94) into t-SNARE. The titration with Vc generated a large heat signal, which gave an affinity constant, K_D, of about 440 *nM* and ΔH of about -19.1 $kcal \cdot mol^{-1}$ (Figure 1C, Supporting Table S1). The reaction between CDV and t-SNARE generated more heat, with ΔH about -40.1 $kcal \cdot mol^{-1}$ and K_D about 130 *nM* (Figure 1D). Because the generated heat is additive, ΔH of Vn binding to t-SNARE equals ΔH of CDV binding minus that of Vc. Thus, the reaction of Vn binding with t-SNARE corresponds to $\Delta H \sim$ -21 $kcal \cdot mol^{-1}$, which seems to contradict the experiment in Figure 1B, in which Vn peptide was titrated into t-SNARE and did not produce any heat signal.

This apparent contradiction may be due to kinetic effects. To test this hypothesis, we mutated Vn, Vc, and CDV to contain a single cysteine residue in their sequences and labeled them with a fluorescent dye. We then monitored fluorescence anisotropy during their binding with t-SNARE. We found that Vn or Vc alone could bind t-SNARE. However, the rate of Vn assembling was much slower (Figure 1E, Supporting Figure S1A). We evaluated the on-rates and affinity

constants of Vn, Vc and CDV binding to t-SNARE (Figures 1E, 1F, S1; Supporting Table S2). These results showed that Vn, Vc, and CDV were all able to bind t-SNARE with similar K_D (85 *nM* for Vn, 170 *nM* for Vc, and 110 *nM* for CDV, Figure 1F). The striking difference is that Vn assembled with t-SNARE much slower than Vc and CDV. The on-rates for Vc and CDV assembly were similar, 6,000 to 7,000 $M^{-1}s^{-1}$; whereas Vn assembled with t-SNARE at an on-rate of only about 500 $M^{-1}s^{-1}$.

Reorganization of the N-terminal three-helix bundle of the t-SNARE is required to accommodate the v-SNARE

To investigate the molecular basis of the kinetically unfavorable N-terminal assembly, we preincubated t-SNARE with Vc peptide. Vc prebound t-SNARE and formed a partial complex at their C-termini, leaving the N-terminus of t-SNARE available for Vn assembly. After the prebinding reached equilibrium, this t-SNARE/Vc mixture was titrated with Vn peptide (Figure 2A). Large heat spikes due to Vn assembling with t-SNARE were measured, with ΔH about -20.2 $kcal \cdot mol^{-1}$, which was consistent the ΔH value calculated above, and K_D about 7 *nM*. The agreement in ΔH suggests that the interactions between the binding residues on Vn and t-SNARE are not altered by Vc. Therefore, it seems that the prebinding of Vc to t-SNARE accelerated the N-terminal assembly of SNAREs.

We then used fluorescence anisotropy to measure the assembly kinetics of Vn binding to t-SNARE that was prebound with Vc (Supporting Figure S2A). We determined the on-rate and found that it was increased by ~1,000 fold, to $4.9*10^5$ $M^{-1}s^{-1}$ (Figure 2B). Hence the previous kinetically unfavorable N-terminal assembly became highly favorable when t-SNARE was prebound with Vc. We also obtained the affinity constant from anisotropy measurements, K_D ~ 5.6 *nM* (Figure 2C). Hence, the binding affinity of N-terminal assembly was improved from 85 nM to 5.6 nM upon Vc addition.

To test whether this prebinding induced activation is limited to Vn peptide, we used the cytosolic domain of v-SNARE (CDV, VAMP2 residue 1 to 94) and similar results were obtained (Supporting Text and Figure S3). The changes in the kinetic and thermodynamic parameters of CDV assembling with t-SNARE upon prebinding are close to those of Vn assembling. This suggests that, in both cases, activation originates from the same underlying molecular mechanism.

Previously, Melia et al reconstituted full length t-SNARE and v-SNARE onto liposomes, respectively, and found that Vc peptide accelerated the rate of lipid mixing between t-SNARE liposomes and v-SNARE liposomes.(11) Here we monitored both content mixing and lipid mixing using nanodiscs and liposomes. The results showed that both lipid mixing and content release were accelerated (~ 10 fold) through preincubating Vc peptide with t-SNARE liposomes (Figures 2D, 2E and 2F), consistent with previous reports.(11, 13)

Fusion between v-SNARE nanodiscs and prebound t-SNARE liposomes is a result of the N- to C- directional zippering: assembly is initialized on their N-termini, followed by displacing the Vc peptide, and assembly continues on the C-termini toward the transmembrane domains to induce bilayer merging. Since the N-terminal assembly of the SNAREs is intrinsically slow and can be significantly accelerated by Vc prebinding, the activation of liposome-nanodisc fusion by Vc is likely due to the acceleration of the N-terminal assembly.

Prebinding of t-SNARE with Vc is not physiologically meaningful as VAMP2 is not present in the plasma membrane prior to docking. However, other factors such as R-SNAREs (proteins containing a VAMP-like domain (VLD) with an Arginine residue on the ionic layer) are in the plasma membrane and may play a similar role as that observed *in vitro* with Vc. Here, to check this general concept, we tested an R-SNARE,Tomosyn, which is found in the cytosol and the plasma membrane.(23) Here we purified a C-terminal peptide of Tomosyn-1 (TSc, residues 1076 to 1115, Supporting Figure S4A).

We first titrated TSc into the solution of the cytosolic domain of t-SNARE, and found that TSc bound t-SNARE with a decent affinity (K_D about 248 *nM*, Supporting Figure S4B). Then we preincubated t-SNARE with TSc, and titrated Vn into this mixture (Figure 3A). The resulting thermograph showed that Vn assembled with prebound t-SNARE with a K_D ~13.6 *nM* and ΔH ~ -20.3 $kcal.mol^{-1}$. In fluorescence anisotropy measurements, Vn assembled rapidly with t-SNARE that was prebound with TSc, with an on-rate k_{on} *of* about $5.1\times10^5\ M^{-1}s^{-1}$ (Figure 3B). In lipid mixing fusion assays, when t-SNARE liposomes were preincubated with TSc, fusion with v-SNARE liposomes was accelerated about 8 fold (Figure 3C). These results show that, similarly to Vc, prebinding of TSc activates the t-SNARE and facilitates the N-terminal assembly. This suggests that such an activation effect is a general feature of the R-SNAREs.

These results show that (i) the N-terminal assembly of SNAREs is intrinsically slow, but can be significantly accelerated to satisfy synaptic vesicle docking/priming when t-SNARE is prebound

with Vc or TSc; (ii) the N-terminal assembly is enthalpy driven and thermodynamically favorable; and (iii) N-terminal assembly is the limiting factor in fusion assays and acceleration of fusion is the direct result of activation on the N-terminal assembly.

A previous study suggested that the function of Vc is to prevent a second Syntaxin binding to the t-SNARE which forms 2:1 (Syntaxin:SNAP25 molar ratio) dead-end complex.(13) Our experimental data have proven that the co-expressed t-SNARE, which was used in our study, contains Syntaxin and SNAP25 at 1:1 molar ration, and Vc accelerates the assembly of t- and v-SNARE even when SNAP25 is in large excess (Supporting Text, Supporting Figure S5). Thus, the action of Vc goes beyond merely preventing dead-end complex formation, but induces a more profound change in t-SNARE. In the following we will show that this change is related to a structural optimization of the t-SNARE.

The SNARE motif of the t-SNARE contains one helix from Syntaxin and two helices from SNAP25; it exhibits a 3-helix-bundle structure on its N-terminus and unstructured on its C-terminus.(14, 24, 25) However, the structure of the postfusion SNARE complex exhibits 4-helix-bundle structure on both its N- and C-termini (Figure 4A).(26) Therefore, during the N- to C-directional zippering process, t-SNAREs must restructure their 3-helix-bundles to accept the 4^{th} helix from VAMP2 to form the 4-helix bundle. Such helix reorganization costs energy. This is key to understanding the molecular basis of Vc accelerating the N-terminal assembly. In a previous study, we observed that when t-SNARE was prebound with a Vn peptide, X-ray crystallography showed a four-helix-bundle structure on its N-terminus and such 4-helix configuration propagates to its C- terminus, even though only three helices existed on the C-terminus.(12, 19) This is the helix continuation model. We hypothesize that, similarly, when Vc binds to t-SNARE, the C-terminus of the SNARE complex is prestructured and adopts the 4-helix-bundle conformation which is able to propagate and disrupt the initial 3-helix bundle on the N-terminus to form the same “4-helix-like” bundle structure as in the full-assembled SNARE (Figure 4A). This prestructuring of the N-terminal region of the SNARE domain is validated by CD spectra, which show that t-SNARE has similar helical content when it is bound with either Vc or Vn peptide (Figure 4B). Thus, a binding site is created on t-SNARE to facilitate the assembly with the N-terminus of v-SNARE. Such preformed binding site must occur prior to N-terminal assembly of the ternary complex to bypass the energy-costly reorganization of the t-SNARE, and hence reduces the kinetic barrier (Figure 4C).

Therefore our data reveal that prebinding with the C-terminal peptide of an R-SNARE not only prestructures t-SNARE's C-terminus, but also reorganizes its N-terminal 3 helices to create a preformed binding site for VAMP2. This provides the molecular basis for the facilitation of N-terminal assembly.

Energy landscape of SNAREpin assembly under zero force

Synaptic vesicle fusion is driven by the C-terminal assembly of the SNAREs, while vesicle docking and priming result from the N-terminal association. Thus determining energy barriers during N- and C-terminal assembly is critical for understanding the kinetics of vesicle priming and fusion.

We performed fluorescence anisotropy measurements to monitor labeled Vn peptide assembling with t-SNARE or t-SNARE preincubated with Vc, at different temperatures T (Supporting Figures S2&S6). We then obtained the on-rate k_{on}, affinity constant K_D, and the off-rate k_{off} (through $K_D = k_{on}/k_{off}$,) at each temperature (Supporting Table S2). Using the classical Arrhenius' equation, $k = Ae^{-E_a/(k_BT)}$, where A is the pre-exponential factor, k_B is the Boltzmann constant, we plotted k_{on} as a function of $1/T$ to obtain the activation barrier of the assembly reaction, $E_{a,\,on}$, both in the absence and presence of Vc prebinding (Figure 5A). The striking finding here is that the activation barrier of the N-terminal assembly is extremely high, $E_{a,\,on} \sim 34\ k_BT$. This is the energy cost of prestructuring t-SNARE by opening the N-terminal 3-helix bundle of t-SNARE to form a 4-helix bundle with the N-terminal subdomain of v-SNARE. This high energy barrier is the reason why the N-terminal assembly is intrinsically slow and needs to be accelerated. In contrast, when t-SNARE is prebound with Vc, the energy barrier is substantially reduced to $E_{a,\,on} \sim 8.6\ k_BT$. As shown above, this large energy reduction is because such prebinding already opens the N-terminal 3-helix bundle into a 4-helix-bundle-like configuration, and this explains why Vc accelerates N-terminal assembly.

Similarly, we plotted k_{off} as a function of $1/T$ to obtain the activation barrier of the disassociation, $E_{a,\,off}$ (Figure 5B). As expected, the energy difference between the two states (Vn assembled state and unassembled state), $E_{a,\,off}$ - $E_{a,\,off}$, is not altered by the prebinding: ~ 16 k_BT both in the presence or absence of the prebinding. Hence prebinding of Vc only changes the activation energy.

Via the same approach, we determined the energy barrier of the C-terminal assembly. We obtained $E_{a,\,on} \sim 13\ k_BT$ for the C-terminal association. We also preincubated t-SNARE with a Vn peptide, and measured the anisotropy of labeled Vc during its assembly with the prebound t-SNARE, and obtained $E_{a,\,on} \sim 4.7\ k_BT$ (Figure 5C and 5D). Similarly, the energy barrier of C-terminal assembly was also largely decreased when t-SNARE is prebound. Prebinding Vn only changes the activation energies but not the energy difference, 18 k_BT, between the Vc unbound and Vc bound states.

For both energy barriers (N-terminal assembly and C-terminal assembly), the difference between the activation energies of the forward and backward reactions are very close to the free energy variations measured by ITC and fluorescence anisotropy. Even though this similarity is not a proof *per se*, it suggests that the energy barriers are not enthalpies but actual free energies.

With the activation barriers of both N- and C-terminal assemblies, we constructed an energy landscape to account for the N- to C- directional zippering (Figure 5E). Due to topological constraints, C-terminal zippering occurs after N-terminal zippering, and hence the assembly substrate is the half-zippered SNARE intermediate. Therefore, the energy barrier of C-terminal assembly is reduced to 4.7 k_BT which allows rapid zippering to satisfy sub-millisecond fast fusion. If t-SNARE is not activated for the N-terminal assembly, the energy landscape of the zippering pathway is described by the blue solid line in Figure 5E. The energy barrier is high, 34 k_BT. When t-SNARE is activated upon prebinding with the C-terminal peptide of an R-SNARE, the energy landscape can be depicted by the red solid line in Figure 5E. Here the barrier for N-terminal association is largely reduced to 8.6 k_BT, so that fast vesicle docking/priming becomes possible. There is an energy minimum between the two kinetic barriers, indicating the existence of the half-zippered SNARE intermediate (zippered on the N-termini but not on the C-termini).

DISCUSSION

Zippering of the t- and v-SNARE is required for membrane fusion. We have quantified the two main energy barriers that dictate the kinetics of this assembly. Our results provide critical insight to the understanding of two physiological processes: the refilling of the readily releasable pool (RRP) and the organization of the regulatory machinery prior to fusion.

SNARE N-terminal assembly must be accelerated for rapid RRP refilling

Due to topological constraints, the folding pathway of the SNAREs starts at their N-termini. N-terminal assembly initializes their association, and primes them by introducing a structural change in t-SNARE.(12) As such, N-terminal assembly is part of the refilling process of the RRP. However, the assembly of these subdomains alone is the limiting step in SNARE zippering with an on-rate of 1900 $M^{-1}s^{-1}$ at 37ºC. The density of SNAREs near the active zone of presynaptic membrane can be estimated to be of the order of ~100 μM, assuming that the gap between two synaptic vesicles prior to refilling the RRP is equal to their diameter (27, 28) and 70 copies of VAMP2 per vesicle (29). The resulting characteristic time is of the order of 10 *s*. This is too slow compared to the expected rate of refilling of the RRP (100 *ms*). Even though N-terminal assembly is energetically favorable, the three-helix bundle that composes the t-SNARE has to be opened and reorganized to accommodate the fourth helix coming from the v-SNARE. This generates a high kinetic energy barrier, 34 k_BT. We propose three non-mutually exclusive scenarios to accelerate the assembly of the N-terminal domains as follows.

First, we have observed that when R-SNARE like peptides are bound to t-SNARE, this reorganization of the three-helix bundle is already achieved before association with v-SNARE. The result is a faster assembly of the N-terminal subdomains with an on-rate of $6.7\text{x}10^5$ $M^{-1}s^{-1}$. Assuming 100 μM concentration, this would correspond to a characteristic time of 15 *ms*, consistent with a fast refilling of the RRP. Hence, we speculate that, *in vivo*, t-SNARE must also be prepared to accept the N-terminal subdomain of v-SNARE by opening up the groove where the fourth helix is inserted. Although full length R-SNARE may occupy the entire SNARE motif of the t-SNARE and inhibit SNARE assembly, studies using the superior cervical ganglion neurons and the insulin-secreting cell line have revealed that Tomosyn enhances the formation of the SNARE complex, increases the fusion-competent readily releasable pool of synaptic vesicles and enhances neurotransmitter release.(30, 31) Yamamoto et al reported that the tail domain of Tomosyn binds the N-terminal half of Tomosyn's VLD, and proposed that after PKA phosphorylation, the tail domain may be able to occupy the N-terminal half, so that only the C-terminal half of the VLD will be available to bind with the t-SNARE.(32) Hence it is possible that this reorganization of t-SNARE may be achieved by an R-SNARE such as Tomosyn, or possibly, any other appropriate peptide in the vicinity of the plasma membrane, through interactions with other factors. Since these peptides are never present alone *in vivo*, such

mechanism requires that the N-terminal region of the VLD is blocked by another factor or template such as Tomosyn's tail domain or Munc18, leaving only the C-terminal region accessible.

Alternately, Munc18 are known to facilitate SNARE assembly.(33, 34) X-ray crystallography showed that Vps33, the Sec1/Munc18 subunit in yeast, binds v-SNARE.(35) It is probable that Munc18 binds VAMP2 and Syntaxin1A simultaneously, which would artificially increase their local concentrations. If this increase is beyond 100 *mM*, N-terminal assembly becomes fast enough to be with the time-frame of RRP refilling. Hence, Munc18 may act as a scaffold to facilitate the formation of the half zippered SNARE.

The third scenario follows a recent suggestion that the t-SNARE is initially not assembled (36). It would only assemble upon binding with VAMP2. In this case, the kinetics may be different from what we observe here.

Pause in the half-zippered state under zero-force

in vivo and *in vitro* studies show that the machinery that regulates fusion seems to act on partial SNARE assembly,(7-10, 17, 19, 37) for instance, studies on the cleavage of VAMP2 by tetanus toxin and Botulinum/B neurotoxin(7) and exocytosis measurements in adrenal chromaffin cells with overexpressed VAMP2 mutants(10) indicated the likelihood of partially folded intermediates. Surface force measurements indicated that partially-zippered SNAREs were stable without any applied force.(21, 38) Optical tweezers experiments observed an intermediate state when force of ~17 *pN* was applied. However, extrapolating the energy landscape to zero-force, the intermediate state disappeared.(15) We recently discovered distinct functional roles for N- and C-terminal zippering.(12) These observations led to the conclusion that the regulatory machinery is set in place when the SNAREpin is kinetically trapped in the half-zippered state. Hence, it is surprising that this state vanishes under zero force. Here, we have unambiguously established this intermediate state exists with an energy barrier of ~5 k_BT (Figure 5E), which corresponds to a lifetime of ~1 μs.(39)

What is the origin of this contradiction? We propose that it can be due to an entropic effect. Indeed, in the optical tweezers experiments, the SNAREs are initially in the folded state and open up due to the stretching force field, and their entropy has been reduced close to the folded state. In contrast, in the present study, the SNAREs initially are in their relaxed, unperturbed

state, and possess their relaxation entropy. Modeling the unstructured SNAREs as polymers, we find that this entropy can bring a few k_BT per SNARE that may be sufficient to account for the 5 k_BT activation energy we measured (See Supporting Text).

Assuming that the kinetic pause between N-terminal and C-terminal assemblies is around 1 μs would suggest that the intermediate state is very transient. Intermembrane repulsions due to the SNAREs themselves or other molecules will increase the duration of this state. However, negative regulators are needed to arrest the half-zippered state and clamp C-terminal assembly. Complexin has been reported to block progression of zippering.(18, 19, 37) The k_{on} of Complexin binding to SNAREs is ~3x10^7 $M^{-1}s^{-1}$ and its concentration is estimated in the 1–2 mM range.(19, 40) Thus, if the intermembrane repulsion is large enough to prolong the lifetime of the intermediate state to ~20 μs, it is possible to recruit Complexin to half-zippered SNARE. Another possible scenario is that Complexin is recruited through binding with t-SNARE before association with v-SNARE, as we previously reported.(17)

In vivo, sequential vesicle docking/priming and fusion are respectively governed by the assembly of the N- and C-terminal subdomains of SNAREs. The intrinsic high energy barrier with N-terminal assembly and subsequent low barrier in the C-terminal subdomain make it possible to enable or inhibit the docking/priming and fusion independently by utilizing regulatory machineries to manipulate the assembly of SNAREs. Both phenomena are essential for precise spatial and temporal regulation of neurotransmission.

MATERIALS AND METHODS

Below is a very brief description of the methods that were used. More details are given in the Supporting Information.

Protein constructs, expression and purification

Proteins were produced by expression in the BL-21 gold (DE3) Escherichia coli bacterial strain, and purified as described before.

Lipid-mixing fusion assay

Lipid mixing between FLT-liposomes and FLV-liposomes was measured by monitoring the dequenching of the DPPE-NBD fluorescence resulting from its dilution into the fused liposomes.

Isothermal Titration Calorimetry (ITC) measurements

ITC experiments were performed with a Microcal ITC200 instrument similarly to that was described before.

Fluorescence Anisotropy

Fluorescence anisotropy was measured using T-format polarization. To obtain the kinetic parameters, we used the equations develop in previous publication.(12)

SUPPORTING INFORMATION

Supporting Text, Figures S1-S7, Table S1-S2, and Methods.

AUTHOR CONTRIBUTIONS

F.L. designed and performed the experiments. F.L. and F.P. analyzed the data. F.L., F.P. and J.E.R. interpreted the results. F.L. and F.P. wrote the paper.

ACKNOWLEDGMENTS

This work was supported by US National Institutes of Health (NIH) grant DK027044 to J.E.R. and French Agence Nationale de la Recherche (ANR) grant ANR- 12-BSV5-0002 to F.P. We thank Dr. T. Melia for providing reagents and many helpful discussions.

REFERENCES

1. Jahn R & Fasshauer D (2012) Molecular machines governing exocytosis of synaptic vesicles. *Nature* 490(7419):201-207.
2. Sudhof TC (1995) The synaptic vesicle cycle: a cascade of protein-protein interactions. *Nature* 375(6533):645-653.
3. Pyle JL, Kavalali ET, Piedras-Renteria ES, & Tsien RW (2000) Rapid reuse of readily releasable pool vesicles at hippocampal synapses. *Neuron* 28(1):221-231.
4. Dittman JS & Regehr WG (1998) Calcium dependence and recovery kinetics of presynaptic depression at the climbing fiber to Purkinje cell synapse. *The Journal of neuroscience : the official journal of the Society for Neuroscience* 18(16):6147-6162.
5. Crowley JJ, Carter AG, & Regehr WG (2007) Fast vesicle replenishment and rapid recovery from desensitization at a single synaptic release site. *The Journal of neuroscience : the official journal of the Society for Neuroscience* 27(20):5448-5460.
6. Moser T & Beutner D (2000) Kinetics of exocytosis and endocytosis at the cochlear inner hair cell afferent synapse of the mouse. *Proceedings of the National Academy of Sciences of the United States of America* 97(2):883-888.
7. Hua SY & Charlton MP (1999) Activity-dependent changes in partial VAMP complexes during neurotransmitter release. *Nature neuroscience* 2(12):1078-1083.
8. Xu T*, et al.* (1999) Inhibition of SNARE complex assembly differentially affects kinetic components of exocytosis. *Cell* 99(7):713-722.
9. Sorensen JB*, et al.* (2006) Sequential N- to C-terminal SNARE complex assembly drives priming and fusion of secretory vesicles. *The EMBO journal* 25(5):955-966.

10. Walter AM, Wiederhold K, Bruns D, Fasshauer D, & Sorensen JB (2010) Synaptobrevin N-terminally bound to syntaxin-SNAP-25 defines the primed vesicle state in regulated exocytosis. *The Journal of cell biology* 188(3):401-413.
11. Melia TJ*, et al.* (2002) Regulation of membrane fusion by the membrane-proximal coil of the t-SNARE during zippering of SNAREpins. *The Journal of cell biology* 158(5):929-940.
12. Li F*, et al.* (2014) A Half-Zippered SNARE Complex Represents a Functional Intermediate in Membrane Fusion. *Journal of the American Chemical Society* 136(9):3456-3464.
13. Pobbati AV, Stein A, & Fasshauer D (2006) N- to C-terminal SNARE complex assembly promotes rapid membrane fusion. *Science* 313(5787):673-676.
14. Fiebig KM, Rice LM, Pollock E, & Brunger AT (1999) Folding intermediates of SNARE complex assembly. *Nature structural biology* 6(2):117-123.
15. Gao Y*, et al.* (2012) Single reconstituted neuronal SNARE complexes zipper in three distinct stages. *Science* 337(6100):1340-1343.
16. Weber JP, Reim K, & Sorensen JB (2010) Opposing functions of two sub-domains of the SNARE-complex in neurotransmission. *The EMBO journal* 29(15):2477-2490.
17. Li F*, et al.* (2011) Complexin activates and clamps SNAREpins by a common mechanism involving an intermediate energetic state. *Nature structural & molecular biology* 18(8):941-946.
18. Giraudo CG*, et al.* (2009) Alternative zippering as an on-off switch for SNARE-mediated fusion. *Science* 323(5913):512-516.
19. Kummel D*, et al.* (2011) Complexin cross-links prefusion SNAREs into a zigzag array. *Nature structural & molecular biology* 18(8):927-933.
20. Wang J*, et al.* (2014) Calcium sensitive ring-like oligomers formed by synaptotagmin. *Proc Natl Acad Sci USA* 111(38):13966-13971.
21. Li F*, et al.* (2007) Energetics and dynamics of SNAREpin folding across lipid bilayers. *Nature structural & molecular biology* 14(10):890-896.
22. Fasshauer D, Sutton RB, Brunger AT, & Jahn R (1998) Conserved structural features of the synaptic fusion complex: SNARE proteins reclassified as Q- and R-SNAREs. *Proceedings of the National Academy of Sciences of the United States of America* 95(26):15781-15786.
23. Fujita Y*, et al.* (1998) Tomosyn: a syntaxin-1-binding protein that forms a novel complex in the neurotransmitter release process. *Neuron* 20(5):905-915.
24. Fasshauer D & Margittai M (2004) A transient N-terminal interaction of SNAP-25 and syntaxin nucleates SNARE assembly. *The Journal of biological chemistry* 279(9):7613-7621.
25. Munson M & Hughson FM (2002) Conformational regulation of SNARE assembly and disassembly in vivo. *The Journal of biological chemistry* 277(11):9375-9381.
26. Sutton RB, Fasshauer D, Jahn R, & Brunger AT (1998) Crystal structure of a SNARE complex involved in synaptic exocytosis at 2.4 A resolution. *Nature* 395(6700):347-353.
27. Fernandez-Busnadiego R*, et al.* (2013) Cryo-electron tomography reveals a critical role of RIM1alpha in synaptic vesicle tethering. *J Cell Biol* 201(5):725-740.
28. Cole AA, Chen X, & Reese TS (2016) A Network of Three Types of Filaments Organizes Synaptic Vesicles for Storage, Mobilization, and Docking. *J Neurosci* 36(11):3222-3230.
29. Takamori S*, et al.* (2006) Molecular anatomy of a trafficking organelle. *Cell* 127(4):831-846.
30. Baba T, Sakisaka T, Mochida S, & Takai Y (2005) PKA-catalyzed phosphorylation of tomosyn and its implication in Ca2+-dependent exocytosis of neurotransmitter. *The Journal of cell biology* 170(7):1113-1125.
31. Cheviet S*, et al.* (2006) Tomosyn-1 is involved in a post-docking event required for pancreatic beta-cell exocytosis. *Journal of cell science* 119(Pt 14):2912-2920.
32. Yamamoto Y*, et al.* (2010) The tail domain of tomosyn controls membrane fusion through tomosyn displacement by VAMP2. *Biochemical and biophysical research communications* 399(1):24-30.
33. Shen J, Tareste DC, Paumet F, Rothman JE, & Melia TJ (2007) Selective activation of cognate SNAREpins by Sec1/Munc18 proteins. *Cell* 128(1):183-195.
34. Voets T*, et al.* (2001) Munc18-1 promotes large dense-core vesicle docking. *Neuron* 31(4):581-591.
35. Baker RW*, et al.* (2015) A direct role for the Sec1/Munc18-family protein Vps33 as a template for SNARE assembly. *Science* 349(6252):1111-1114.
36. Ma C, Su L, Seven AB, Xu Y, & Rizo J (2013) Reconstitution of the vital functions of Munc18 and Munc13 in neurotransmitter release. *Science (New York, N.Y* 339(6118):421-425.
37. Cho RW*, et al.* (2014) Genetic Analysis of the Complexin Trans-clamping Model for Cross-linking SNARE Complexes In Vivo. *Proc Natl Acad Sci USA*.

38. Wang YJ, *et al.* (2016) Snapshot of sequential SNARE assembling states between membranes shows that N-terminal transient assembly initializes fusion. *Proc Natl Acad Sci U S A* 113(13):3533-3538.
39. Evans E (2001) Probing the relation between force--lifetime--and chemistry in single molecular bonds. *Annu Rev Biophys Biomol Struct* 30:105-128.
40. Pabst S, *et al.* (2002) Rapid and selective binding to the synaptic SNARE complex suggests a modulatory role of complexins in neuroexocytosis. *Journal of Biological Chemistry* 277(10):7838-7848.
41. Wiederhold K & Fasshauer D (2009) Is assembly of the SNARE complex enough to fuel membrane fusion? *The Journal of biological chemistry* 284(19):13143-13152.

FIGURE LEGENDS

Figure 1. **Thermodynamics and kinetics of SNARE assembly. (A)** Illustration of the structure of the t-SNARE. The SNARE motifs of Syntaxin1A (red) and SNAP25 (green) interact to form a complex. **(B) to (D)** ITC measurements of Vn peptide (**B**), Vc peptide (**C**) and CDV (**D**) assembling with the t-SNARE, respectively. Raw data in power vs. time during the injection was presented in the upper panels. Integrated heat vs. the molar ratio was plotted in the lower panels. The solid lines represented the best fits to the black squares. Thermodynamic parameters were listed in Supporting Table S1. **(E) & (F)** Fluorescence anisotropy experiments were performed to monitor the binding process of Vn (blue triangles), Vc (green circles) and CDV (red squares) to the t-SNARE at various concentrations at 26ºC, respectively. The anisotropy versus time curves were presented in Supporting Figure S1. **(E)** The initial binding rates were plotted versus the concentration of t-SNARE (markers). The solid lines were fits to obtain the on-rates. The error bars were determined from the standard deviation of measurements in the anisotropy. **(F)** Plateau anisotropy values were plotted versus the concentration of t-SNARE (markers). The solid lines were fits to obtain the affinity constants.

Figure 2. **Vc peptide activates N-terminal assembly both kinetically and thermodynamically. (A)** ITC measurements of titration of Vn into prebound t-SNARE. To prebind the Vc peptide, the t-SNARE and Vc peptide (molar ratio 1:8) were incubated together at 37ºC for 60 min prior to titration. **(B)&(C)** Fluorescence anisotropy experiments were performed to monitor the binding process of Vn to prebound t-SNARE at various concentrations at 26ºC. The anisotropy versus time curves were presented in Supporting Figure S2A. Initial binding rates and plateau anisotropy values were plotted versus concentration of t-SNARE, respectively, to obtain the on-rate **(B)** and affinity constant **(C**). The error bars were deermined from the standard

deviation of measurements in the anisotropy. **(D) to (F)** Vc peptide accelerates fusion rate in the content release assay. $CaCl_2$ was encapsulated inside full length t-SNARE-containing liposomes. When liposomes fused with nanodiscs containing full length v-SNARE, $CaCl_2$ was released from liposomes. Signals from both content release **(D)** and lipid mixing **(E)** were measured. When Vc prebound FLT (filled diamonds), both rates were accelerated. Positive control (filled circles) represented fusion of t-liposomes and v-nanodiscs in the absence of prebinding. Negative control (open circles) showed fusion between t-liposomes preincubated with cytosolic VAMP2 (CDV, residues 1-94) and v-nanodiscs. ~10 fold of activation due to prebinding of Vc was observed when compared with positive control **(F)**.

Figure 3. **Tomosyn-1 C-peptide accelerates N-terminal assembly of the SNAREs. (A)** TSc activates the t-SNARE in ITC measurements. ~440 μM Vn peptide was titrated into ~37 μM t-SNARE prebound with TSc. **(B)** Fluorescence anisotropy experiments were performed to monitor the binding process of Vn to t-SNARE prebound with TSc at various concentrations. Initial binding rates were plotted versus the concentration of t-SNARE (filled triangles). The solid lines were fits to obtain the on-rate. **(C)** TSc accelerates fusion rate between t-liposomes and v-liposomes. Rates of lipid mixing were measured in the absence (black filled circles) and presence (pink triangles) of prebinding with TSc. Negative control (black open circles) showed fusion between t-liposomes preincubated with CDV and v-liposomes.

Figure 4. **Molecular basis for activation of the t-SNARE and acceleration of N-terminal assembly. (A)** Helicity continuation model. When a Vn peptide binds the t-SNARE (middle), or a C-terminal peptide of R-SNARE prebinds the t-SNARE (right), both N-terminal and C-terminal domains adopt the same 4-helix bundle structure as in the postfusion, fully-assembled SNARE complex (left). **(B)** Vn and Vc peptides structure the t-SNARE to similar extent. After incubating with Vn or Vc peptide, respectively, the CD spectra of SNAREs exhibited similar amount of helical structure. The CD spectrum of t-SNARE was less structured, and CD spectra of Vn or Vc are largely unstructured. **(C)** Model of the molecular basis for activation of N-terminal assembly. In the N- to C- directional zippering, the N-terminus of the t-SNARE needs to reorganize its 3-helix bundle to accept the 4^{th} helix from the v-SNARE. When a

C-terminal peptide of R-SNARE prebinds the t-SNARE, N-terminus of v-SNARE is able to directly assemble with the preformed site and bypasses the helix reorganization.

Figure 5. **Energy landscape of the kinetic barriers of the N- and C- terminal assemblies. (A) & (B)** Fluorescence anisotropy experiments were performed to monitor the binding process of Vn to the t-SNARE at various concentrations and different temperatures in the absence (blue triangles) or presence (purple diamonds) of prebinding with excessive Vc, respectively. k_{on} and k_{off} were then plot versus $1/T$ to obtain the kinetic energy barriers of N-terminal association **(A)** and disassociation **(B)**, respectively. **(C)&(D)** Fluorescence anisotropy experiments were performed to monitor the binding process of Vc to the t-SNARE in the absence (green circles) or presence (pink diamonds) of prebinding with excessive Vn, respectively. k_{on} and k_{off} were then plot versus $1/T$ obtain the kinetic energy barriers of C-terminal association **(C)** and disassociation **(D)**, respectively. The error bars were determined from the standard deviation of measurements in the anisotropy. (**E**) Energy landscape of the activation barriers. The left side corresponds to the unbound states. The relative positions of the states (corresponding to the two minima in the plot) are free energies directly measured by ITC and florescence anisotropy. The activation energy barriers are determined by varying the temperature in the fluorescence anisotropy assay and may also be free energies (see text). In the absence of activation of the t-SNARE, the zippering pathway follows the blue solid curve. In the presence of activation, the zippering pathway follows the red solid curve. In both situations, the barrier of C-terminal assembly is low (~4.7 k_BT) as N-terminal zippering occurs first, which prestructures the C-terminus of the t-SNARE. The dashed curve indicates the barrier of C-terminal assembly when N-termini are not zippered.

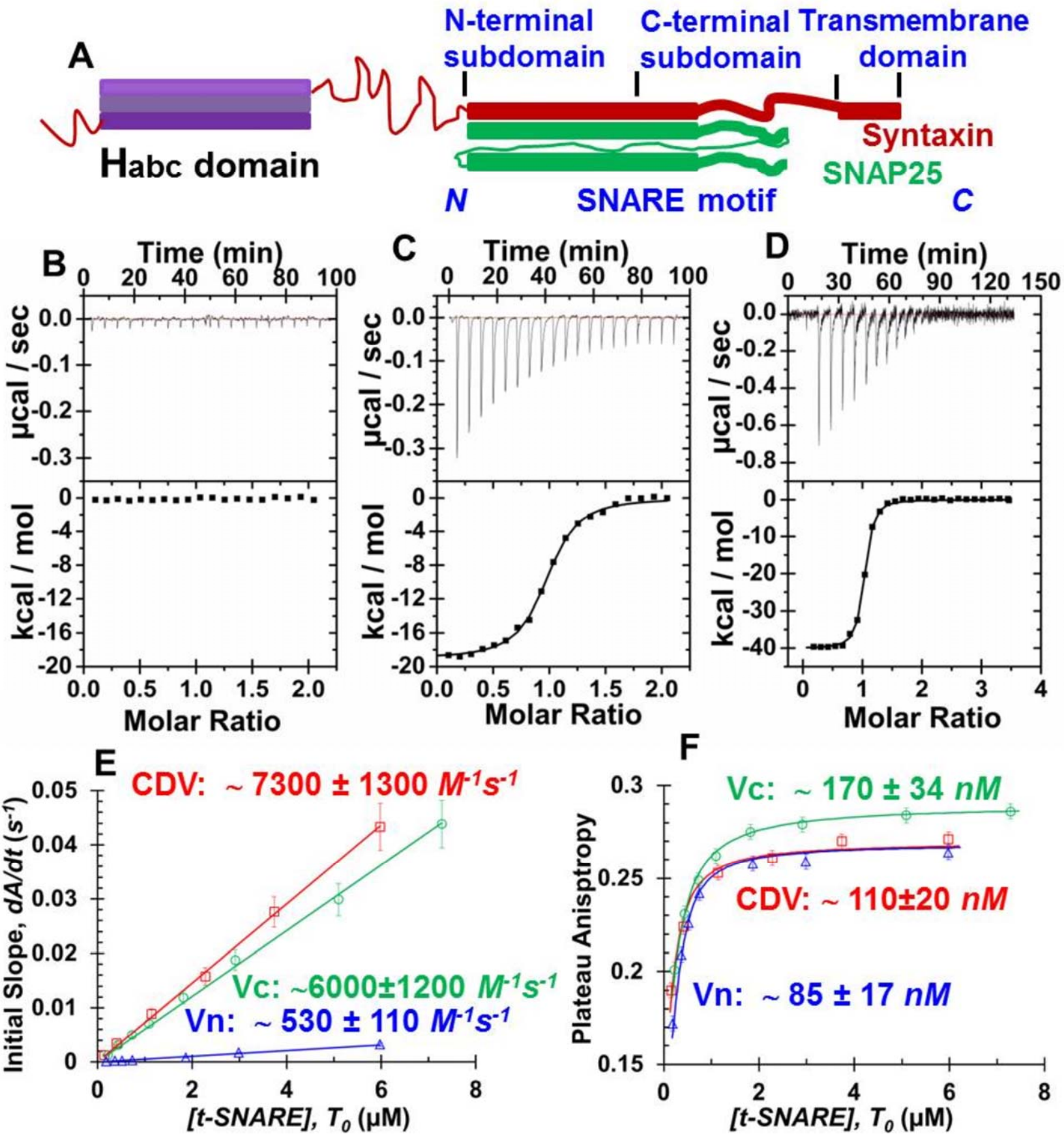
A
N-terminal subdomain
C-terminal subdomain
Transmembrane domain
Habc domain
Syntaxin
SNAP25
N
SNARE motif
C
B
C
D
Time (min)
µcal / sec
kcal / mol
Molar Ratio
E
CDV: ~ 7300 ± 1300 M-1s-1
Vc: ~6000±1200 M-1s-1
Vn: ~ 530 ± 110 M-1s-1
Initial Slope, dA/dt (s-1)
[t-SNARE], T0 (µM)
F
Vc: ~ 170 ± 34 nM
CDV: ~ 110±20 nM
Vn: ~ 85 ± 17 nM
Plateau Anisptropy
[t-SNARE], T0 (µM)

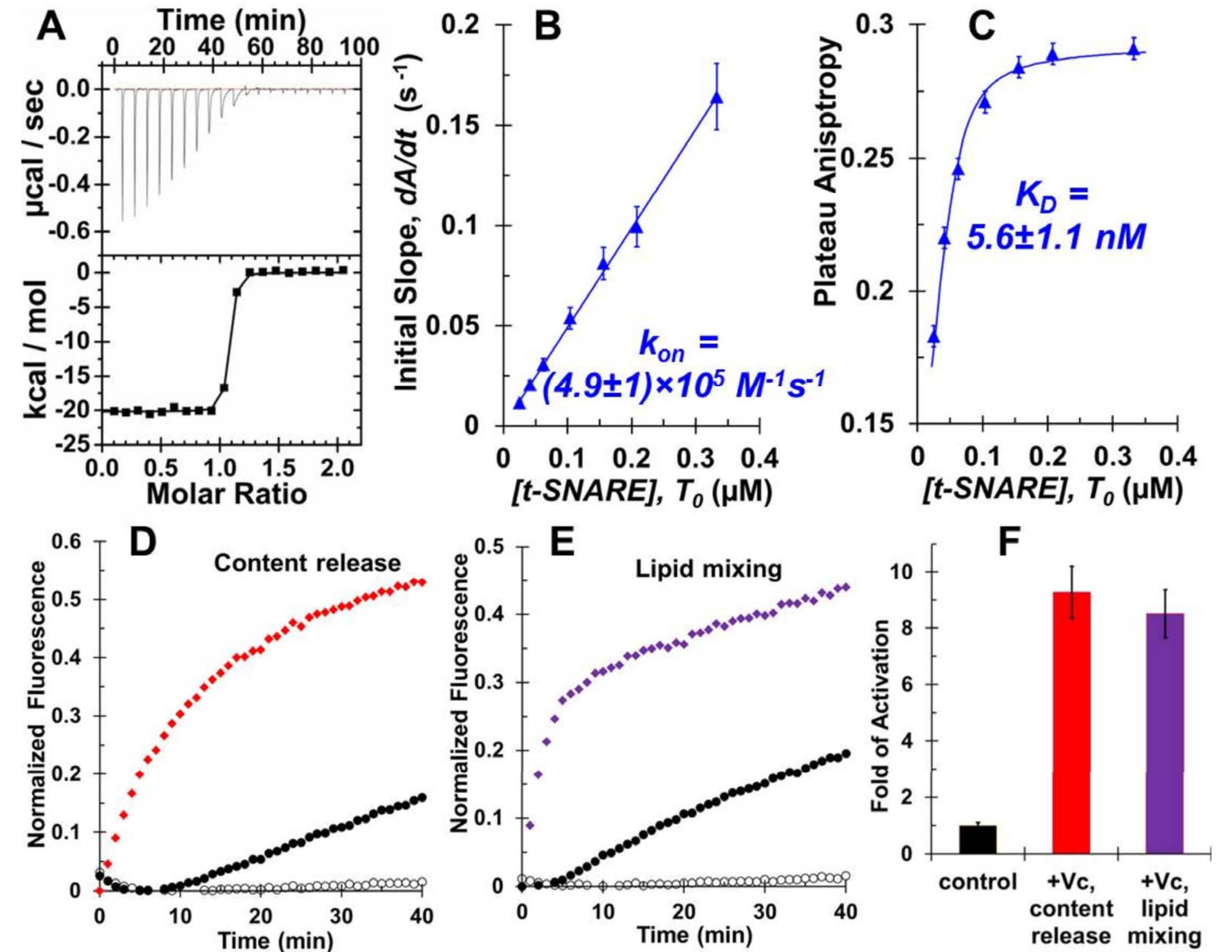
A
Time (min)
0 20 40 60 80 100
µcal / sec
0.0
-0.2
-0.4
-0.6
kcal / mol
0
-5
-10
-15
-20
-25
0.0 0.5 1.0 1.5 2.0
Molar Ratio
B
Initial Slope, dA/dt (s-1)
0.2
0.15
0.1
0.05
0
kon =
(4.9±1)×10^5 M^-1 s^-1
0 0.1 0.2 0.3 0.4
[t-SNARE], T0 (µM)
C
Plateau Anisptropy
0.3
0.25
0.2
0.15
KD =
5.6±1.1 nM
0 0.1 0.2 0.3 0.4
[t-SNARE], T0 (µM)
D
Content release
Normalized Fluorescence
0.6
0.5
0.4
0.3
0.2
0.1
0
0 10 20 30 40
Time (min)
E
Lipid mixing
Normalized Fluorescence
0.5
0.4
0.3
0.2
0.1
0
0 10 20 30 40
Time (min)
F
Fold of Activation
10
8
6
4
2
0
control
+Vc, content release
+Vc, lipid mixing

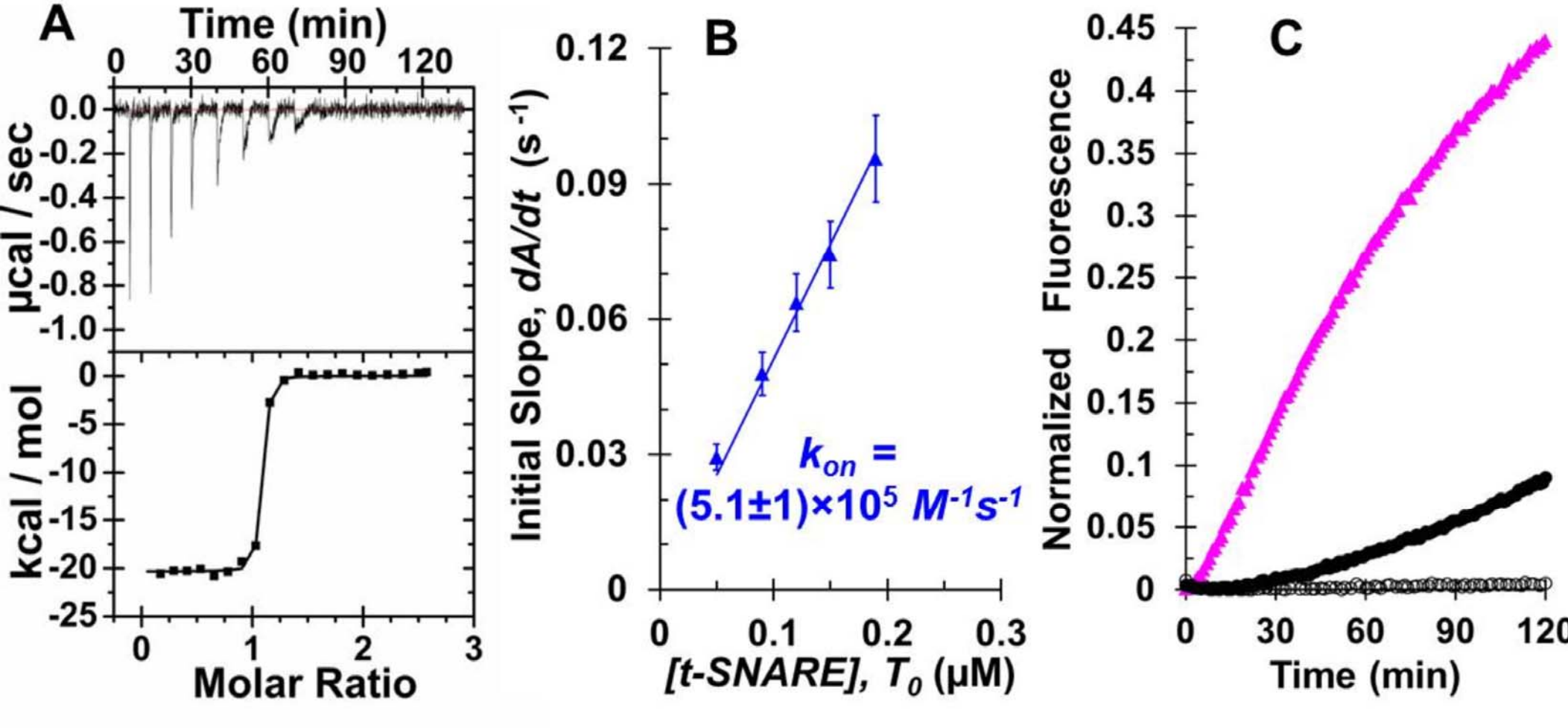
A
Time (min)
0
30
60
90
120
0.0
-0.2
-0.4
-0.6
-0.8
-1.0
µcal / sec
0
-5
-10
-15
-20
-25
kcal / mol
0
1
2
3
Molar Ratio
B
0.12
0.09
0.06
0.03
0
Initial Slope, dA/dt (s-1)
kon =
(5.1±1)×10^5 M-1s-1
0
0.1
0.2
0.3
[t-SNARE], T0 (µM)
C
0.45
0.4
0.35
0.3
0.25
0.2
0.15
0.1
0.05
0
Normalized Fluorescence
0
30
60
90
120
Time (min)

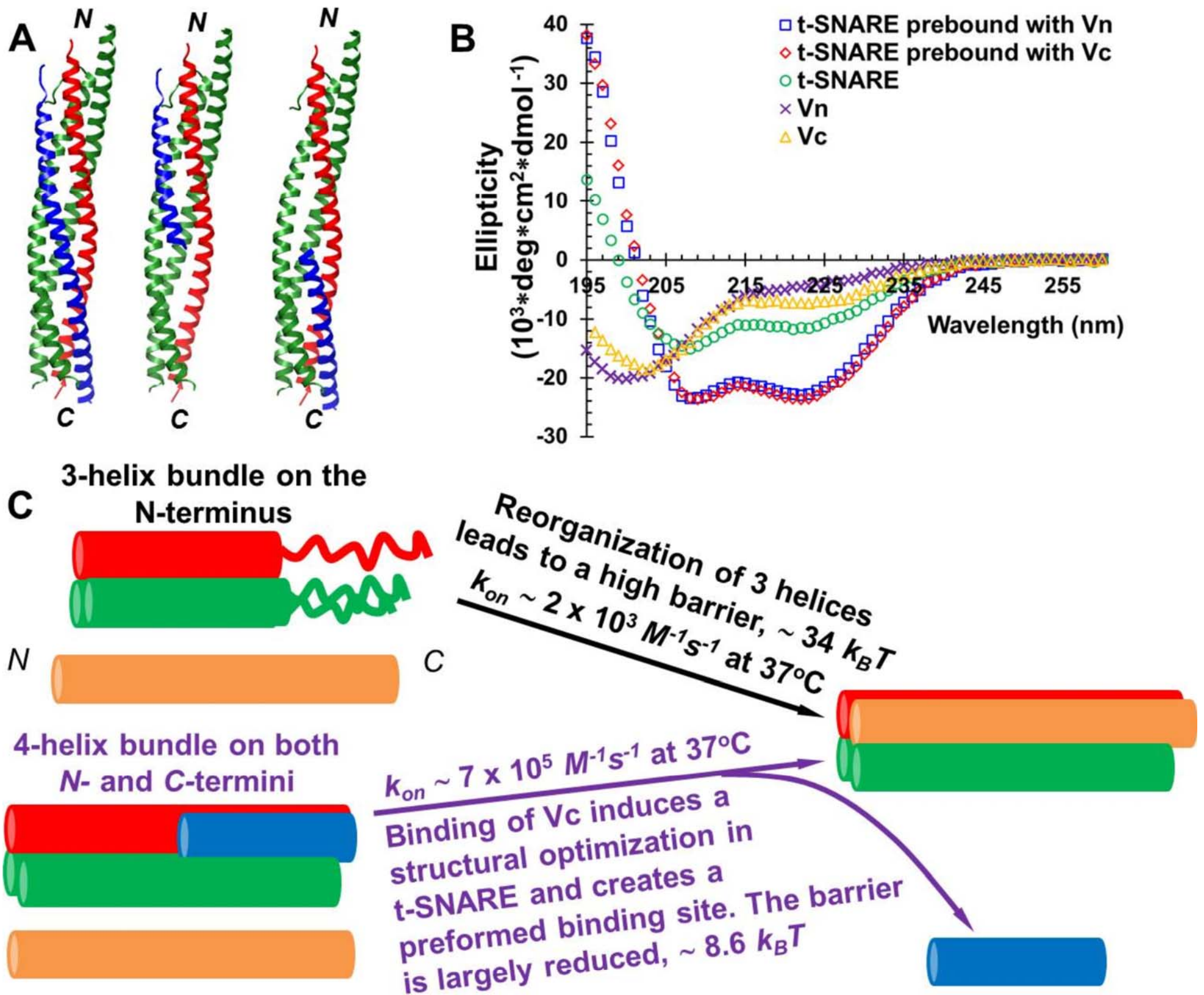
A
N
N
N
C
C
C
B
t-SNARE prebound with Vn
t-SNARE prebound with Vc
t-SNARE
Vn
Vc
Ellipticity
(10³*deg*cm²*dmol⁻¹)
40
30
20
10
0
-10
-20
-30
195
205
215
225
235
245
255
Wavelength (nm)
C
3-helix bundle on the
N-terminus
N
C
Reorganization of 3 helices
leads to a high barrier, ~ 34 k_BT
k_{on} ~ 2 x 10³ $M^{-1}s^{-1}$ at 37°C
4-helix bundle on both
N- and C-termini
k_{on} ~ 7 x 10⁵ $M^{-1}s^{-1}$ at 37°C
Binding of Vc induces a
structural optimization in
t-SNARE and creates a
preformed binding site. The barrier
is largely reduced, ~ 8.6 k_BT

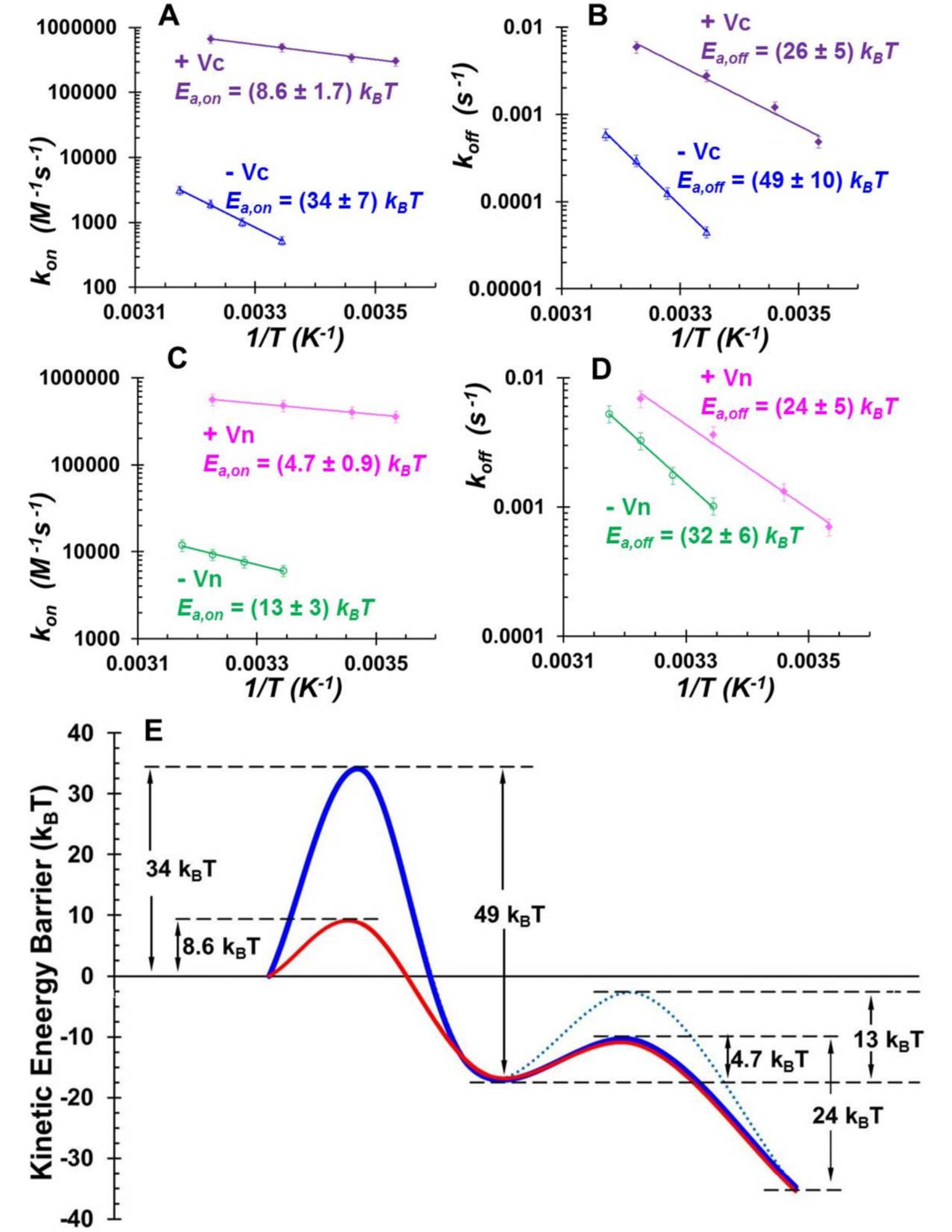
A
+ Vc
$E_{a,on}$ = (8.6 ± 1.7) k_BT
- Vc
$E_{a,on}$ = (34 ± 7) k_BT
k_{on} ($M^{-1}s^{-1}$)
1/T (K^{-1})
B
+ Vc
$E_{a,off}$ = (26 ± 5) k_BT
- Vc
$E_{a,off}$ = (49 ± 10) k_BT
k_{off} (s^{-1})
1/T (K^{-1})
C
+ Vn
$E_{a,on}$ = (4.7 ± 0.9) k_BT
- Vn
$E_{a,on}$ = (13 ± 3) k_BT
k_{on} ($M^{-1}s^{-1}$)
1/T (K^{-1})
D
+ Vn
$E_{a,off}$ = (24 ± 5) k_BT
- Vn
$E_{a,off}$ = (32 ± 6) k_BT
k_{off} (s^{-1})
1/T (K^{-1})
E
Kinetic Eneergy Barrier (k_BT)
34 k_BT
8.6 k_BT
49 k_BT
4.7 k_BT
13 k_BT
24 k_BT